



Published in final edited form as:

*Chem Phys Lett.* 2010 January ; 484(4-6): 304–308. doi:10.1016/j.cplett.2009.12.002.

## Measuring the SERS Enhancement Factors of Dimers with Different Structures Constructed from Silver Nanocubes

Pedro H. C. Camargo, Leslie Au, Matthew Rycenga, Weiyang Li, and Younan Xia\*

Department of Biomedical Engineering, Washington University, St. Louis, MO 63130, USA

### Abstract

We describe a systematic investigation on the SERS enhancement factors of individual dimers ( $EF_{dimer}$ ) constructed from two Ag nanocubes that display a face-to-face, edge-to-face, or edge-to-edge structure. The highest field-enhancements were obtained for the dimers displaying a face-to-face and edge-to-face configuration. In these two systems,  $EF_{dimer}$  was insensitive to the dimer geometry and corresponded to  $2.0 \times 10^7$  and  $1.5 \times 10^7$ , respectively. However,  $EF_{dimer}$  was decreased to  $5.6 \times 10^6$  for the edge-to-edge structure. These variations in the detected field-enhancements could be explained based on the relative orientation of the nanocubes and the number of probe molecules enclosed in the hot-spot region for each dimer configuration.

### 1. Introduction

Surface-enhanced Raman scattering (SERS) is the only technique capable of detecting a single molecule and simultaneously probing its chemical structure [1–5]. It is generally accepted that SERS detection at the single-molecule level requires substrates containing hot spots [6–9], which can be defined as the junctions between two or more closely spaced Ag or Au nanoparticles. In the hot-spot region, extraordinary electromagnetic enhancements could arise as compared to their individual counterparts [10–12]. Although many studies have been devoted to investigation of mechanisms responsible for such giant enhancements, the hot-spot phenomenon is still an allusive and feebly understood subject. As a result, fabrication of SERS substrates for single-molecule detection remains to be an art rather than a science and still has to rely on the random aggregation of Ag or Au colloids as induced by a salt [13].

Dimers consisting of two closely spaced Ag or Au nanoparticles represents a promising alternative for studying the hot-spot phenomenon. As an individual dimer represents the simplest system encompassing a hot spot, it allows one to easily correlate the detected SERS signals with the specific structure of a dimer or hot spot. However, shape irregularity and surface roughness often associated with the nanoparticles employed as building blocks to construct nanoparticle dimers imposes some challenges to precisely calculate the number of molecules being probed and, consequently, the field enhancement from an individual dimer [14–19]. Recently, we have demonstrated the utilization of dimers made of two Ag nanospheres, two sharp Ag nanocubes, and an individual Ag nanowire decorated with a sharp Ag nanocube as substrates for SERS, followed by measurements of their respective enhancement factors (EFs) [20–23]. In our studies, the utilization of well-defined and uniform

\*Corresponding author. xia@biomed.wustl.edu.

**Publisher's Disclaimer:** This is a PDF file of an unedited manuscript that has been accepted for publication. As a service to our customers we are providing this early version of the manuscript. The manuscript will undergo copyediting, typesetting, and review of the resulting proof before it is published in its final citable form. Please note that during the production process errors may be discovered which could affect the content, and all legal disclaimers that apply to the journal pertain.

particles with smooth surfaces was instrumental to a meaningful correlation between the detected SERS intensities or calculated EFs and the specific structure of a dimer or hot spot.

Non-spherical particles containing sharp corners are especially attractive as substrates for SERS. Generally, theoretical calculations predict that nanoscale sharp features can provide stronger Raman scattering intensities than rounded counterparts as they allow for a higher concentration of near fields (lightning rod effect) [24–27]. Also, the utilization of non-spherical particles to construct dimers enables one to obtain dimeric systems displaying a variety of structures and thus hot-spot morphologies. However, there has been very few experimental investigations with regard to how different nanoparticle arrangements (and thus hot-spot morphologies) would affect the experimentally detected SERS intensities and the corresponding EFs of individual dimers [23,28]. Such an investigation would be attractive not only for a better understanding of the hot-spot phenomenon, but also from a practical aspect, allowing the maximization of SERS signals coming from a dimer upon the optimization of its structure. For dimers constructed from an individual nanowire decorated with a sharp nanocube, for example, we found that the specific orientation of the Ag nanocube with respect to the nanowire's side face played a pivotal role in enhancing the SERS signals [23].

Here we report a systematic study of the SERS activities of dimers constructed from two sharp Ag nanocubes displaying a variety of well-defined structures. Specifically, we investigated three distinct dimer structures: *i*) two sharp Ag nanocubes with side faces nearly touching each other; *ii*) a sharp Ag nanocube having one edge nearly touching the face of another sharp Ag nanocube; and *iii*) a sharp Ag nanocube having one edge nearly touching the edge of another sharp Ag nanocube. In these systems, the hot spot region can be described as the narrow gap between: *i*) two flat faces of the two nanocubes (face-to-face); *ii*) an edge and a flat face of the two nanocubes (edge-to-face); and *iii*) two edges of the two nanocubes (edge-to-edge). By measuring the EFs of these dimeric structures ( $EF_{dimer}$ ), we were able to evaluate how the dimer morphology affects  $EF_{dimer}$  relative to the individual nanocubes.

## 2. Experimental details

### 2.1. Chemicals and materials

Silver nitrate ( $AgNO_3$ , 99%), poly(vinyl pyrrolidone) (PVP, Mw 55,000), hydrochloric acid (HCl, 37% in water) and 4-methylbenzenethiol (4-MBT, 98%) were all obtained from Sigma-Aldrich and used as received. Ethylene glycol (EG) was obtained from J. T. Baker, and ethanol (200 proof) was obtained from Pharmco Products. All aqueous solutions were prepared with deionized water (18.1 M $\Omega$  cm).

### 2.2. Synthesis of Ag nanocubes

The Ag nanocubes were synthesized according to our previously reported protocols [29,30]. In a typical synthesis, 5 mL of EG was placed in a 20-mL vial, capped, and heated with magnetic stirring in an oil bath at 150 °C for 1 h. 0.75 mL of 12 mM HCl in EG was then quickly added into the vial, and the vial was recapped. After 10 min, 1.5 mL each of 94 mM  $AgNO_3$  and 147 mM PVP (calculated in terms of the repeating unit), both dissolved in EG, were simultaneously added through a two-channel syringe pump (KDS-200, KD Scientific, Holliston, MA) at a rate of 22.5 mL/h into the vial. The vial was then capped and continued with heating at 150 °C until the solution turned into an ocher color. Upon injection of the  $AgNO_3$  solution, the reaction mixture went through a series of color changes that included milky white, light yellow, transparent, red, and ocher. The final product, silver nanocubes with sharp corners, was obtained by centrifugation (30 min at 3,900 rpm) and washed with acetone once and ethanol twice to remove excess EG and PVP and finally re-dispersed in ethanol for further use in the preparation of SERS substrates.

### 2.3. Preparation of substrates for correlated SERS/SEM experiments

Samples for correlated SEM and SERS experiments were prepared by drop-casting an ethanol suspension of the Ag nanocubes on a Si substrate that had been patterned with registration marks and letting it dry under ambient conditions. In this case, dimers with different structures could form spontaneously via aggregation during solvent evaporation. Functionalization with 4-MBT was performed by immersing the substrate containing Ag nanocubes in a 5 mM ethanol solution (5 mL) of 4-MBT for 1 h. The sample was then taken out, washed with copious amounts of ethanol, and finally dried under a stream of air. All samples were used immediately for SERS measurements after preparation.

### 2.4. Instrumentation

The SERS spectra were recorded using a Renishaw inVia confocal Raman spectrometer coupled to a Leica microscope with a 50× objective (NA = 0.90) in the backscattering geometry. The 514 nm wavelength was generated with an argon laser coupled to a holographic notch filter with a grating of 1200 lines per millimeter. While we have a 785 nm wavelength laser this was not used in this experiment with the single cube or the different dimers due to the low SERS signal reported with this excitation. This low signal is presumably due to the lack of coupling of the LSPR to the excitation, as these structures have LSPRs closer to 514 nm and not 785 nm [20]. The backscattered Raman signals were collected on a thermoelectrically cooled (−60 °C) CCD detector. The scattering spectra were recorded in the range of 800–2000  $\text{cm}^{-1}$ , in one acquisition of 30 s accumulation, and 0.5 mW at the sample. In the spectra, the broad band at 900–1000  $\text{cm}^{-1}$  can be attributed to the Si substrate and was used in this work as a reference for intensity normalization. SEM images were taken using an FEI field-emission microscope (Nova NanoSEM 230) operated at an accelerating voltage of 15 kV.

### 2.5. Calculation of the Enhancement Factor (EF)

We employed the peak at 1582  $\text{cm}^{-1}$  to estimate the EF through the following equation:

$$EF = (I_{\text{sers}} \times N_{\text{normal}}) / (I_{\text{normal}} \times N_{\text{sers}}) \quad (1)$$

where  $I_{\text{sers}}$  and  $I_{\text{normal}}$  are the intensities of the same band for the SERS and normal Raman spectra,  $N_{\text{normal}}$  is the number of molecules probed for a normal Raman setting, and  $N_{\text{sers}}$  is the number of molecules probed in SERS. The areas of the 1582  $\text{cm}^{-1}$  band were used for the intensities  $I_{\text{sers}}$  and  $I_{\text{normal}}$ . We chose this band because it was the strongest band in the spectra.  $N_{\text{normal}}$  was determined based on the Raman spectrum of a 0.1 M 4-MBT solution in 12 M  $\text{NaOH}_{(\text{aq})}$  and the focal volume of our Raman system (1.48  $\mu\text{L}$ ). When determining  $N_{\text{sers}}$ , we assumed that the 4-MBT molecules were adsorbed as a monolayer with a molecular footprint of 0.19  $\text{nm}^2$  [31,32]. This assumption represents the theoretically maximum number of molecules and is therefore an overestimate. Thus, the calculated EF will likely be an underestimate rather than an overestimate of the enhancement. As 4-MBT does not present any absorption bands matching the laser wavelength used in this study, any possibility of resonance Raman effects can be ruled out from the calculated EFs.

## 3. Results and discussion

Figure 1 shows a SEM image of the sharp Ag nanocubes employed in our SERS studies. They had an edge length of  $100.7 \pm 5.7$  nm. Owing to their well-defined shapes, smooth surfaces and sharp corners, they are ideal building blocks for fabricating dimers with a variety of structures. We employed 4-MBT molecules as the probe for SERS because they are known to form well-defined a monolayer on the silver surface with a characteristic molecular footprint, which is

crucial to estimating the total number of molecules being probed during the SERS measurement and, therefore, a precise estimate of the EF.

We started our studies by evaluating the SERS activity of the Ag nanocubes. Figure 2A shows the SERS spectrum recorded for an aqueous solution of Ag nanocubes that had been functionalized with 4-MBT. The 4-MBT intense and characteristic peaks at 1072 and 1582  $\text{cm}^{-1}$  could be easily resolved in the spectrum [33,34]. Here, the peak at 1072  $\text{cm}^{-1}$  is due to a combination of the phenyl ring-breathing mode, CH in-plane bending, and CS stretching (7a vibrational mode), while the peak at 1582  $\text{cm}^{-1}$  can be assigned to phenyl ring stretching motion (8a vibrational mode) [33,34]. The peaks at 1184, 1377, 1486 and 1695 can be assigned to in-plane phenyl ring vibrations (9a, 3, 3 and 8a vibrational modes, respectively) [33,34]. The EF for the nanocubes calculated from this solution phase spectrum corresponded to  $2.1 \times 10^6$ , which is in agreement with their morphology characterized by relatively large sizes and sharp corners [24].

Figure 2B shows typical SERS spectra for a single Ag nanocube supported over a Si substrate under two laser polarization directions: along a face diagonal and along an edge (top and bottom traces, respectively). The characteristic 4-MBT peaks at 1072 and 1582  $\text{cm}^{-1}$  could be observed for both spectra [33,34]. The broad band at 900–1000  $\text{cm}^{-1}$  originated from the Si substrate. The SERS spectra from the Ag nanocubes presented a strong dependence on laser polarization, which is consistent with our previous reports and is due to the difference in the near-field distribution over the surface of a Ag nanocube under different excitation directions.<sup>35</sup> The 4-MBT signals were more strongly enhanced when the nanocube was oriented with one of its face diagonals parallel to the laser polarization direction. The EF for the Ag nanocube ( $EF_{cube}$ ) was  $3.0 \times 10^6$  and  $5.8 \times 10^5$  for laser polarization along a face diagonal and an edge, respectively. These values are in agreement with the EF calculated from the solution phase spectrum (Fig. 2A). As an approximation, if we take the average of the EF values obtained from laser polarization along a face diagonal and an edge, for example,  $EF_{cube}$  becomes  $1.8 \times 10^6$ , which is close to the  $2.1 \times 10^6$  value obtained from the solution phase spectrum. It is important to note that the nanocubes are expected to display random orientations with respect to the laser excitation polarization direction for the SERS spectrum recorded in the solution phase. Thus, the EF calculated from the solution measurement represents an average value for all possible orientations of the Ag nanocubes relative to the laser polarization direction.

After the SERS spectra for an individual nanocube had been investigated, we turned our attention to dimers composed of two Ag nanocubes displaying a *i*) face-to-face, *ii*) edge-to-face, or *iii*) edge-to-edge configuration. Figure 3A shows the SERS spectra taken for individual dimers displaying the aforementioned structures and the insets show their corresponding SEM images. Here, the laser was polarized parallel to the dimer's longitudinal axis, i.e., parallel to the hot-spot region. Under this condition, the characteristic 4-MBT SERS signals were significantly enhanced as compared to Figure 2 due to the formation of a hot spot. The EF for the dimers ( $EF_{dimer}$ ) under this laser polarization direction was calculated as  $2.0 \times 10^7$ ,  $1.5 \times 10^7$ , and  $5.6 \times 10^6$  for the face-to-face, edge-to-face and edge-to-edge structures, respectively. According to these results, the highest field-enhancements were obtained for the dimers displaying face-to-face and edge-to-face configuration. Interestingly, the detected field-enhancements were insensitive with respect to the face-to-face and edge-to-face dimer configurations (they presented very similar  $EF_{dimer}$ ). Conversely, when the dimer displayed an edge-to-edge geometry,  $EF_{dimer}$  was decreased by 3.6 and 2.7 folds relative to the face-to-face and edge-to-face structures, respectively.

It is well-established that, in dimers made of two nearly touching Ag nanoparticles, the calculated  $EF_{dimer}$  represents an average enhancement from all probe molecules adsorbed in/on the dimer, i.e., from probe molecules both within and outside the hot-spot region [3–7]. In

principle, for a given dimeric system, a higher number of probe molecules adsorbed in the hot-spot region ( $N_{hot-spot}$ ) is expected to lead to stronger SERS intensities and thus a higher  $EF_{dimer}$ . Figure 4 shows a schematic representation of dimers probed in Figure 3 and their respective hot-spot morphologies. Based on the molecular footprint of 4-MBT and the dimensions of the Ag nanocubes,  $N_{hot-spot}$  was calculated as 105,263, 10,210 and 5,894 for the face-to-face, edge-to-face and edge-to-edge structures, respectively. Our results show that the dimers displaying a face-to-face and edge-to-face configuration presented similar SERS activities despite the fact that the edge-to-face orientation leads to a  $\sim 10$  folds decrease in  $N_{hot-spot}$ . In this dimer, it is possible that the decrease in  $N_{hot-spot}$  was compensated by the higher SERS activity of the one nanocube having its face diagonal parallel to the laser polarization direction under the edge-to-face configuration. It is important to note that, as shown in Figure 2B for a single Ag nanocube,  $EF_{cube}$  was increased by 5.2 folds when the laser excitation was polarized along a face diagonal as compared to polarization along an edge. In the edge-to-edge geometry, however,  $N_{hot-spot}$  and  $EF_{dimer}$  were decreased by  $\sim 18$  and 3.6 folds with respect to the face-to-face configuration. Here, the higher SERS activity provided by the two nanocubes oriented with a face diagonal parallel to the laser polarization direction was not large enough to completely compensate the reduction in  $N_{hot-spot}$ , thus leading to an overall decrease in  $EF_{dimer}$ . It is worth mentioning that the calculated  $EF_{dimer}$  corresponded to a 28, 9, and 2 folds increase with respect to  $EF_{cube}$  for the face-to-face, edge-to-face, and edge-to-edge configurations, respectively. As the  $N_{hot-spot}$  increases in the order of face-to-face > edge-to-face > edge-to-edge, this observation suggests that a higher relative increase in  $EF_{dimer}$  with respect to  $EF_{cube}$  was observed for dimer configurations that allow for a higher  $N_{hot-spot}$ . This result agrees with the increased contribution of the probe molecules adsorbed in the hot-spot region to the overall field-enhancements for the dimers, relative to their individual nanocubes counterparts, as  $N_{hot-spot}$  increases.

Figure 3B shows the SERS spectra obtained for the dimers presenting a face-to-face, edge-to-face and edge-to-edge configuration in which the laser was polarized perpendicular to the longitudinal axis in the dimers, i.e., perpendicular to the hot-spot axis. It can be observed that the intensities of the SERS signals were significantly decreased for all dimers as compared to those in Figure 3A. Here,  $EF_{dimer}$  was calculated as  $6.6 \times 10^5$ ,  $1.9 \times 10^6$ , and  $3.0 \times 10^6$  for the face-to-face, edge-to-face and edge-to-edge structure, respectively. We also note here that the error associated with the  $EF_{dimer}$  measurement was near 30%, so our comparisons between dimer configurations are statistically significant. The highest  $EF_{dimer}$  were obtained for the edge-to-edge and edge-to-face configurations. However, in all cases, the calculated  $EF_{dimer}$  were within the same order of magnitude as their corresponding constituent particles, suggesting that the molecules adsorbed in the hot-spot region did not make any additional contribution towards the EFs when the laser was polarized perpendicular to the hot-spot axis. Figure 5 summarizes the EFs obtained for the individual Ag nanocubes and their respective dimers probed in Figure 3. For all dimers, the highest field-enhancements were obtained for polarization parallel to the dimer's longitudinal axis. At this polarization, the near-field distribution is expected to be concentrated along the hot-spot region, leading to increased SERS intensities as compared to the individual nanocubes. However, when the laser polarization direction was perpendicular to the dimer's longitudinal axis, the near field distribution should be concentrated outside the hot-spot region. Thus, no coupling between the near fields from the two nearly touching nanocubes takes place and the  $EF_{dimer}$  values fall to the same order of magnitude as  $EF_{cube}$ .

#### 4. Conclusions

We have measured the SERS EFs for dimers constructed from two sharp Ag nanocubes presenting a variety of well-defined structures. In particular, we have investigated three distinct dimer structures: *i*) two sharp Ag nanocubes with side faces nearly touching each other (face-

to-face); *ii*) a sharp Ag nanocube having one edge nearly touching the face of another sharp Ag nanocube (edge-to-face); and *iii*) a sharp Ag nanocube having one edge nearly touching the edge of another sharp Ag nanocube (edge-to-edge). A stronger field enhancement was detected when the laser was polarized parallel to (rather than perpendicular to) the hot-spot axis. Moreover, the strongest field enhancement was obtained for the dimer displaying a face-to-face or edge-to-face structure. In these cases,  $EF_{dimer}$  was calculated as  $2.0 \times 10^7$  and  $1.5 \times 10^7$ , respectively. Conversely,  $EF_{dimer}$  was  $5.6 \times 10^6$  when the dimer presented an edge-to-edge arrangement, representing a decrease of 3.6 folds as compared to the face-to-face configuration. These variations in  $EF_{dimer}$  were explained based on the relative orientation of the nanocubes and the number of probe molecules in the hot-spot region for each dimer configuration. The results presented herein indicate that, for dimers constructed from two nearly touching non-spherical nanoparticles, the optimization of the dimer structure can provide another venue for the maximization of their corresponding SERS activities. In dimers constructed from two sharp Ag nanocubes, the highest SERS activities could be obtained when the nanocubes are arranged either in a face-to-face or in an edge-to-face orientation with respect to each another.

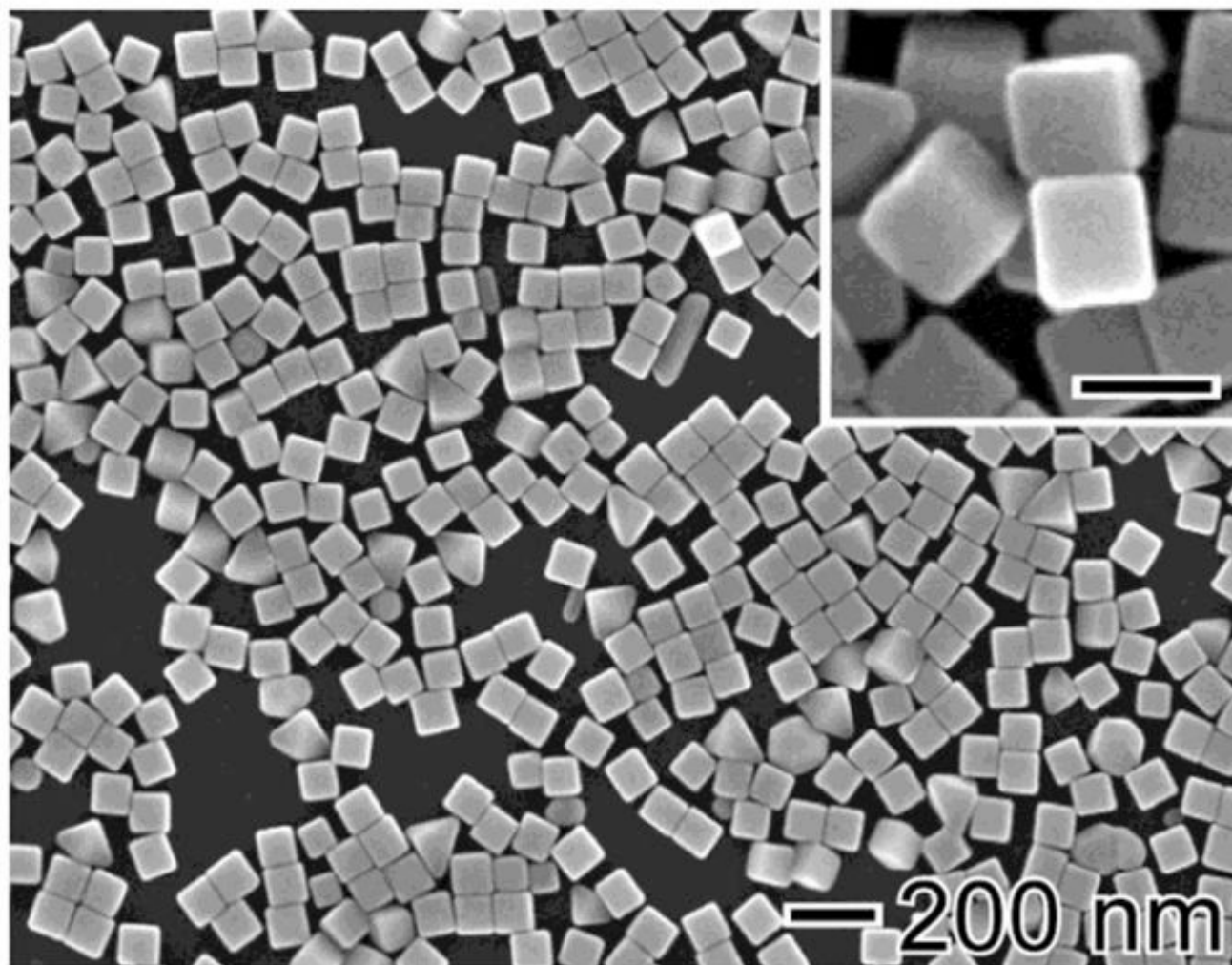
## Acknowledgments

This work was supported in part by a research grant from the NSF (DMR-0804088) and a 2006 Director's Pioneer Award from the NIH (DPI OD000798). P.H.C.C. was supported in part by the Fulbright Program and the Brazilian Ministry of Education (CAPES). Part of the work was performed at the Nano Research Facility (NRF), a member of the National Nanotechnology Infrastructure Network (NNIN), which is supported by the National Science Foundation under NSF award no. ECS-0335765. NRF is part of School of Engineering and Applied Science at Washington University in St. Louis.

## References

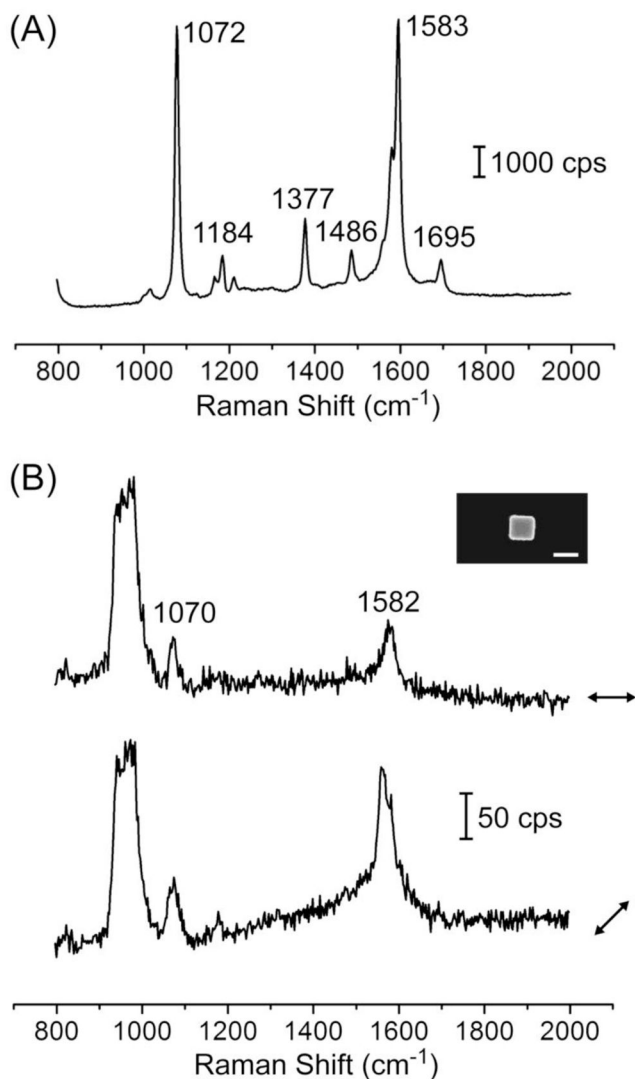
1. Nie S, Emory SR. *Science* 1997;275:1102. [PubMed: 9027306]
2. Kneipp K, Wang Y, Kneipp H, Perelman LT, Itzkan I, Dasari RR, Feld MS. *Phys Rev Lett* 1997;78:1667.
3. Kneipp K, Kneipp H. *J Kneipp Acc Chem Res* 2006;39:443.
4. Stiles PL, Dieringer JA, Shah NL, R P Van Duyne *Annu Rev Anal Chem* 2008;1:601.
5. Pieczonka NPW, Aroca RF. *Chem Soc Rev* 2008;37:946. [PubMed: 18443680]
6. Le Ru EC, Etchegoin PG, Meyer M. *J Phys Chem* 2006;125:104701.
7. Otto AJ. *J Raman Spectrosc* 2006;37:937.
8. Doering WE, Nie S. *J Phys Chem B* 2002;106:311.
9. Etchegoin PG, Le Ru EC. *Phys Chem Chem Phys* 2008;10:6079. [PubMed: 18846295]
10. Le Ru EC, Meyer M, Blackie E, Etchegoin PG. *J Raman Spectrosc* 2008;39:1127.
11. Le Ru EC, Blackie E, Meyer M, Etchegoin PG. *J Phys Chem C* 2007;111:13794.
12. Otto A. *J Raman Spectrosc* 2002;33:593.
13. Kneipp K, Kneipp H, Itzkan I, Dasari RR, Feld MS. *Chem Rev* 1999;99:2957. [PubMed: 11749507]
14. Olk P, Renger J, Härtling T, Wenzel MT, Eng LM. *Nano Lett* 2007;7:1736. [PubMed: 17497823]
15. Svedberg F, Li Z, Xu H, Käll M. *Nano Lett* 2006;6:2639. [PubMed: 17163680]
16. Talley CE, Jackson JB, Oubre C, Grady NK, Hollars CW, Lane SM, Huser TR, Nordlander P, Halas NJ. *Nano Lett* 2005;5:1569. [PubMed: 16089490]
17. Camden JP, Dieringer JA, Wang Y, Masiello DJ, Marks LD, Schatz GC, Van Duyne RP. *J Am Chem Soc* 2008;130:12616. [PubMed: 18761451]
18. Hutchison JA, Centeno SP, Odaka H, Fukumura H, Hofkens J, Uji-i H. *Nano Lett* 2009;9:995. [PubMed: 19199757]
19. Lee SJ, Baik JM, Moskovits M. *Nano Lett* 2008;8:3244. [PubMed: 18767889]
20. Li W, Camargo PHC, Lu X, Xia Y. *Nano Lett* 2009;9:485. [PubMed: 19143509]
21. Li W, Camargo PHC, Au L, Zhang Q, Xia Y. *Angew Chem Int Ed.* 2009 in press.

22. Camargo PHC, Au L, Xia Y. *Angew Chem Int Ed* 2009;48:2180.
23. Camargo PHC, Cobley C, Rycenga M, Xia Y. *Nanotechnology* 2009;20:434020. [PubMed: 19801754]
24. Rycenga M, Kim MH, Camargo PHC, Cobley C, Li ZY, Xia Y. *J Phys Chem A* 2009;113:3932. [PubMed: 19175302]
25. McLellan JM, Siekkinen A, Chen J, Xia Y. *Chem Phys Lett* 2006;427:122.
26. Kelly K, Coronado E, Zhao L, Schatz GC. *J Phys Chem B* 2003;107:668.
27. Hao E, Schatz GC. *J Chem Phys* 2004;120:357. [PubMed: 15267296]
28. Wei H, Hao F, Huang Y, Wang W, Nordlander P, Xu H. *Nano Lett* 2008;8:2497. [PubMed: 18624393]
29. Skrabalak SE, Au L, Li X, Xia Y. *Nat Protoc* 2007;2:2182. [PubMed: 17853874]
30. Im SH, Lee YT, Wiley B, Xia Y. *Angew Chem Int Ed* 2005;44:2154.
31. Seo K, Borguet E. *J Phys Chem C* 2007;111:6335.
32. Tao Y-T, Wu C-C, Eu J-Y, Lin W-L, Wu K-C, Chen C-H. *Langmuir* 1997;13:4018.
33. Han S, Lee S, Kim K. *Langmuir* 2001;17:6981.
34. Sauer G, Brehm G, Schneider S. *J Raman Spectrosc* 2004;35:568.
35. McLellan JM, Li ZY, Siekkinen AR, Xia Y. *Nano Lett* 2007;7:1013. [PubMed: 17375965]

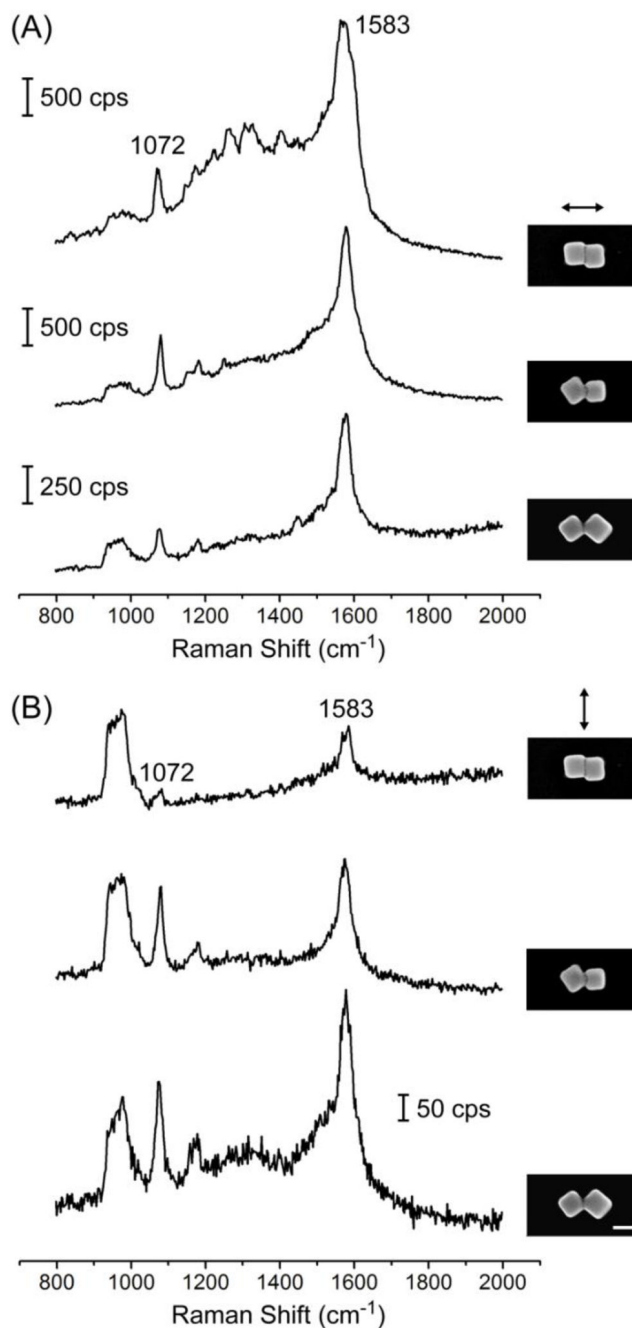


**Figure 1.** SEM image of the Ag nanocubes employed in our SERS measurements. Their average edge length was  $100.7 \pm 5.7$  nm, respectively. The scale bars in the inset correspond to 100 nm.



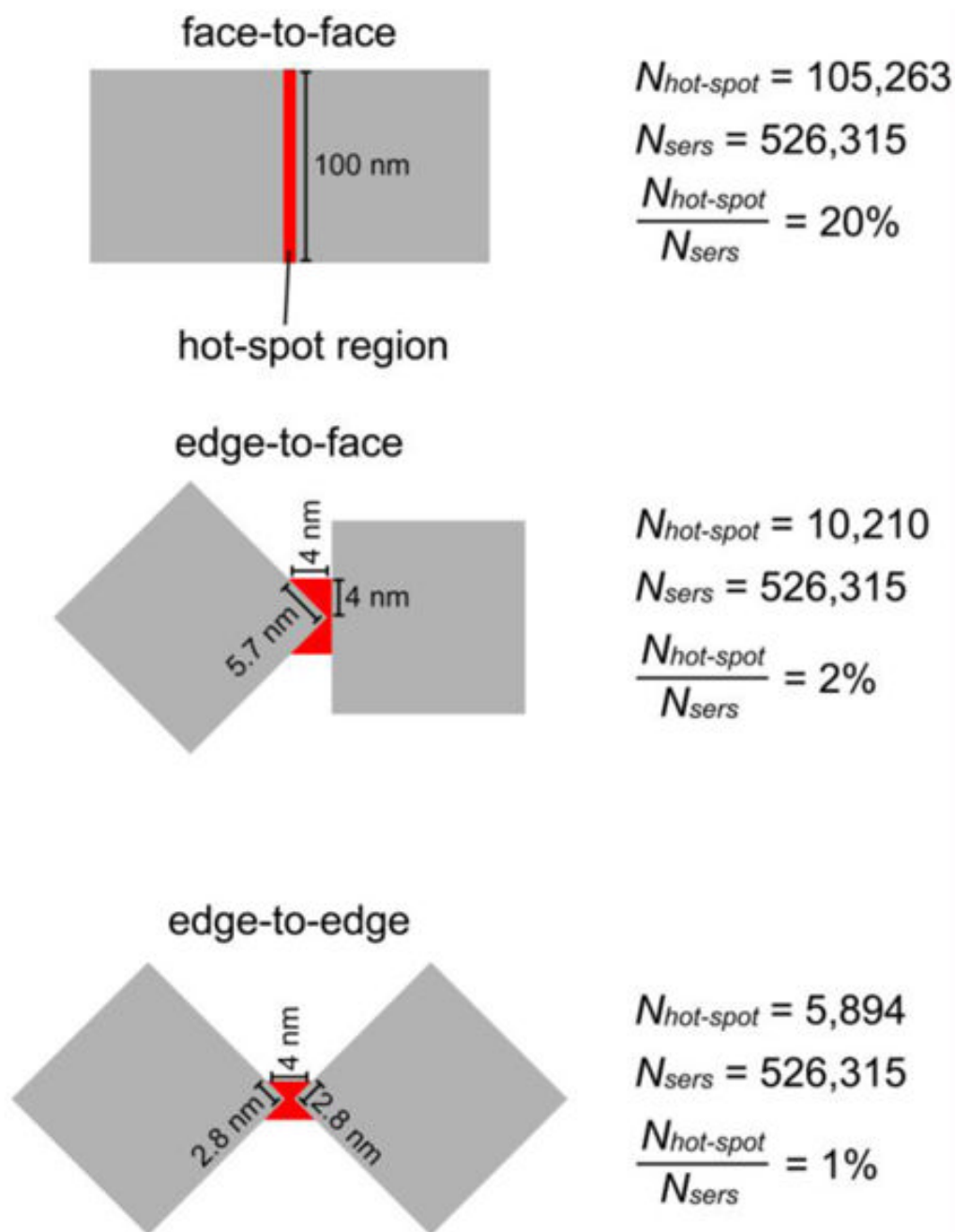


**Figure 2.** (A) SERS spectra recorded from aqueous suspensions of the Ag nanocubes that had been functionalized with 4-MBT.  $EF_{cube}$  calculated from the solution-phase spectra was  $2.1 \times 10^6$ . (B) SERS spectra from a single Ag nanocube deposited over a Si substrate. The sample was functionalized with 4-MBT and the arrows indicate the laser polarization direction relative to the nanocube. Here, the SERS signals were more strongly enhanced when the laser was polarized along a face diagonal (bottom trace). The inset shows an SEM image of the probed Ag nanocube. The scale bar in the inset corresponds to 100 nm.




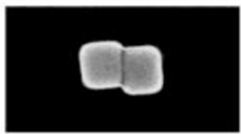
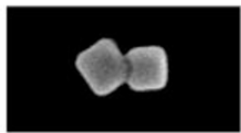
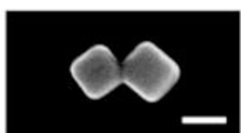
**Figure 3.**

(A, B) SERS spectra for dimers consisting of two sharp Ag nanocubes displaying a variety of well-defined structures: face-to-face (top trace), edge-to-face (middle trace), or edge-to-edge (bottom trace). The samples were functionalized with 4-MBT. The insets display SEM images of the probed dimers. The scale bars applies to all insets and correspond to 100 nm. The double arrows indicate the laser polarization direction in (A) and (B). In (A), the laser was polarized along the longitudinal axis of each dimer. Conversely, the laser was polarized perpendicular to the longitudinal axis of each dimer in (B).



**Figure 4.**

Schematic illustrations (top view) of the dimers probed in Figure 3. The red color marks the hot-spot region for each dimer. In these dimers, the hot-spot region can be described by the narrow gap between: two nearly touching side faces, an edge and a side face, and two nearly touching edges (face-to-face, edge-to-face, and edge-to-edge configurations, respectively).  $N_{hot-spot}$  refers to the number of 4-MBT molecules in the hot-spot region, while  $N_{sers}$  refers to the total number of molecules adsorbed on the entire surface of the dimer.

	Enhancement Factor (EF)
	$\longleftrightarrow 7.2 \times 10^5$ $\nearrow 2.5 \times 10^6$
	$\longleftrightarrow 2.0 \times 10^7$ $\updownarrow 6.6 \times 10^5$
	$\longleftrightarrow 1.5 \times 10^7$ $\updownarrow 1.9 \times 10^6$
	$\longleftrightarrow 5.6 \times 10^6$ $\updownarrow 3.0 \times 10^6$

**Figure 5.**

Summary of the enhancement factors calculated for a single Ag nanocube, and the dimers of nanocubes probed in Figure 3. The highest  $EF_{dimer}$  values were obtained when the laser was polarized parallel to the dimer's longitudinal axis. While the  $EF_{dimer}$  for the face-to-face and edge-to-face configuration were comparable, they corresponded to an increase of 27 and 9 folds with respect to  $EF_{cube}$ , respectively. For the edge-to-face configuration,  $EF_{dimer}$  was within the same order of magnitude as  $EF_{cube}$ . When the laser was polarized perpendicular to the dimer's longitudinal axis, the highest  $EF_{dimer}$  was obtained for the edge-to-edge configuration. However, the  $EF_{dimer}$  was comparable to  $EF_{cube}$  for all dimer structures.